

Movies2Scenes: Learning Scene Representations Using Movie Similarities

Shixing Chen Xiang Hao Xiaohan Nie Raffay Hamid
Amazon Prime Video

{shixic, xianghao, nxiaohan, raffay}@amazon.com

Abstract

Labeling movie-scenes is a time-consuming process which makes applying end-to-end supervised methods for scene-understanding a challenging problem. Moreover, directly using image-based visual representations for scene-understanding tasks does not prove to be effective given the large gap between the two domains. To address these challenges, we propose a novel contrastive learning approach that uses commonly available movie-level information (e.g., co-watch, genre, synopsis) to learn a general-purpose scene-level representation. Our learned representation comfortably outperforms existing state-of-the-art approaches on eleven downstream tasks evaluated using multiple benchmark datasets. To further demonstrate generalizability of our learned representation, we present its comparative results on a set of video-moderation tasks evaluated using a newly collected large-scale internal movie dataset.

1. Introduction

Automatic understanding of scenes (§ 3 for definition) in movies is a challenging problem [50] [25] that offers a variety of applications including video moderation, search and recommendation. The long-form nature of movies makes labeling of their scenes a laborious process. This dearth of scene-level labels makes it challenging to apply end-to-end supervised learning for movie-scene understanding.

The general problem of learning in limited-label settings has been looked at from a variety of alternative perspectives [48], among which contrastive learning [26] has emerged as a particularly promising direction. Specifically, methods that use natural language supervision to guide contrastive learning [38] have shown impressive results specifically for zero-shot image-classification tasks. However, these methods rely on the availability of image-text pairs which are particularly hard to collect for long-form videos. Another important set of methods within the space of contrastive learning focuses on using a *pre-text task* to contrast similar data-points with randomly selected ones [22][9]. However, most of the relatively simple data-augmentation schemes [22] used to define the pre-text tasks for these ap-

proaches have been shown to be not as effective for tasks related to scene understanding [8]. To address these challenges, we propose a novel contrastive learning algorithm to find a general purpose scene-representation that works well for a diverse set of scene-understanding tasks.

Our **key intuition** is that commonly available sources of movie-information (e.g., genre, synopsis, co-watch information) can be used to effectively guide the process of learning a generalizable scene-representation. Specifically, we use such movie-level information to define a measure of movie-similarity, and use it during contrastive learning to limit our search for positive scene-pairs to only the movies that are considered similar to each other. This allows us to find positive scene-pairs that are not only visually similar but are also semantically relevant, and can therefore provide us with a much richer set of geometric and thematic data-augmentations compared to previously employed augmentation schemes [22] [8] (see Figure 1 for illustration). Furthermore, unlike previous contrastive learning approaches that mostly focus on images [22] [9] [13] or shots [8], our approach builds on the recent developments in vision transformers [12] to allow using variable-length multi-shot inputs. This enables our method to seamlessly incorporate the interplay among multiple shots resulting in a more effective and general-purpose scene-representation.

Using a newly collected internal dataset MovieCL30K containing 30,340 movies to learn our scene representation, we demonstrate the flexibility of our approach to handle both individual shots as well as multi-shot scenes as inputs to outperform existing state-of-the-art results on **eleven downstream tasks** using multiple public benchmark datasets [50][25][39]. Moreover, as an important practical application of long-form video understanding, we apply our scene-representation to another newly collected internal dataset MCD focused on large-scale video-moderation with 44,581 video clips from 18,330 movies and TV episodes containing sex, violence, and drug-use activities. We show that learning our general-purpose scene-representation is crucial to recognize such age-appropriate video-content where existing representations learned for short-form action recognition or image classification are not as effective.

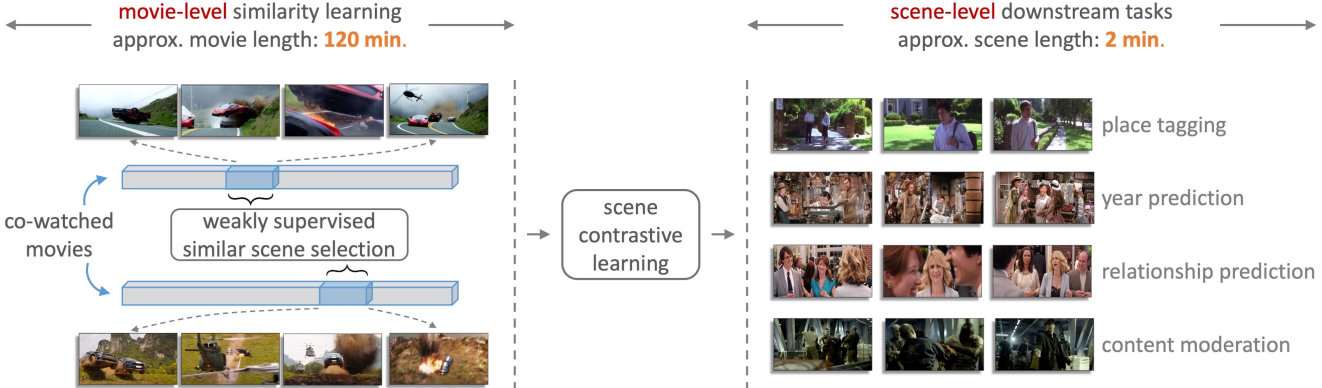


Figure 1: **Approach Overview** – We employ commonly available movie-level information (e.g., co-watch, genre, synopsis) to define movie similarities which are used to learn scene-level representations. The figure illustrates a pair of similar movies where movie similarity is defined based on co-watch information, *i.e.*, viewers who watched one movie often watched the second movie as well. Other movie-level data *e.g.*, genre and synopsis can be also used to define additional movie-level similarities. Our approach automatically selects thematically similar scenes from such similar movie-pairs and uses them in a contrastive learning setting to learn scene-level representations.

2. Related Work

a. Long-Form Video Understanding: Recent work on semantic understanding of long-form movies and TV episodes have used multi-shot scenes as their processing unit. For example in MovieNet [25], manually annotated multi-shot scenes were used to train various recently proposed models [7] [16] to evaluate their performance on multiple tasks related to scene-tagging *e.g.* recognizing places or actions in those scenes. In [35], multi-shot clips of movies and TV episodes were categorized into 25 event-classes for their temporal localization. The results in [35] show that state-of-the-art event localization models [52] [53] do not perform as well on long-form movie and TV episodes compared to their performance on short-form video datasets like THUMOS14 [27]. A long-form video understanding (LVU) dataset was recently proposed in [50] with nine different tasks related to semantic understanding of video-clips that were cut-out from full-length movies. This work also proposed an object-centric transformer-based video recognition architecture that outperformed SlowFast [16] and VideoBert [43] models on their LVU [50] dataset. To compliment existing datasets focusing on regular everyday activity-categories, we use a new internal dataset focusing on video-moderation of sensitive activities including sex, violence, and drug-use, and show how our scene-representation can be applied to recognize these activities.

b. Contrastive Learning: As an important subset of self-supervised learning [28], contrastive learning [31] attempts to learn data representations by contrasting similar data against dissimilar data while using a contrastive loss. Recent approaches for contrastive learning [22] [9] have successfully been extended for a variety of applications in image classification [44] [24] [19] as well as video understanding [21] [8] [55]. More recently, various visio-linguistic

models [38] have adopted natural language supervision during contrastive learning to learn correspondences between image and text pairs, which has achieved impressive results especially for zero-shot image classification tasks. Most of these approaches however focus on images or short-videos, and our experiments show that they do not perform as well on tasks related to long-form video-understanding.

c. Vision Transformer: Derived from the work on self-attention [46], transformers have been extensively studied in natural language processing [49] [11]. Building on this line of work, recently proposed vision transformer (ViT) [12] has successfully exceeded state-of-the-art results when pre-trained on large-scale datasets. The data-efficiency of ViT was recently improved by [45] by using token-based distillation for model training. More recently, ViT-based architectures were adopted to video recognition, with models including TimeSformer [3], ViViT [2], and MViT [14]. These models take images or short-form videos as inputs, and therefore cannot be applied to longer videos without additional tuning.

3. Method

For consistency, let us define a **shot** as a series of frames captured from the same camera over a consecutive period of time [42]. We define a **scene** as a series of consecutive shots without requiring manually annotated scene-boundaries. Note that our definition of scenes is less constrained than what has previously been used [25] [39][8], and enables our approach to work seamlessly with settings that do [25] or do not have [50] scene boundaries available.

Our approach consists of three key steps. First, we use commonly available movie information (*e.g.*, genre, synopsis or co-watch information) to define a measure of movie-level similarity \mathcal{S} (see § 4.1 for details). We use \mathcal{S} as pseudo-labels to train a network that maximizes the simi-

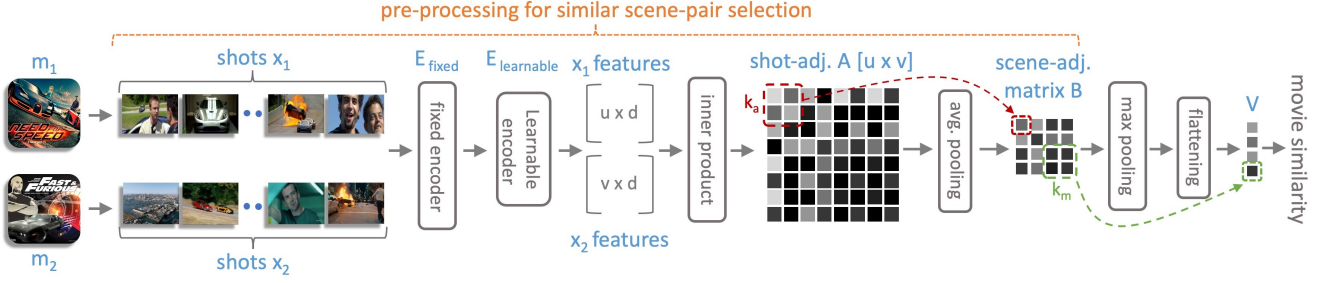


Figure 2: **Movie Similarity Learning** – Shots of a movie-pair m_1 and m_2 are provided to an encoder with fixed parameters (E_{fixed}) followed by an encoder with learnable parameters ($E_{\text{learnable}}$). We take the inner-product of shot-feature matrices followed by successive pooling and flattening operations to get an output vector V which is regressed against movie-level similarity S between m_1 and m_2 .

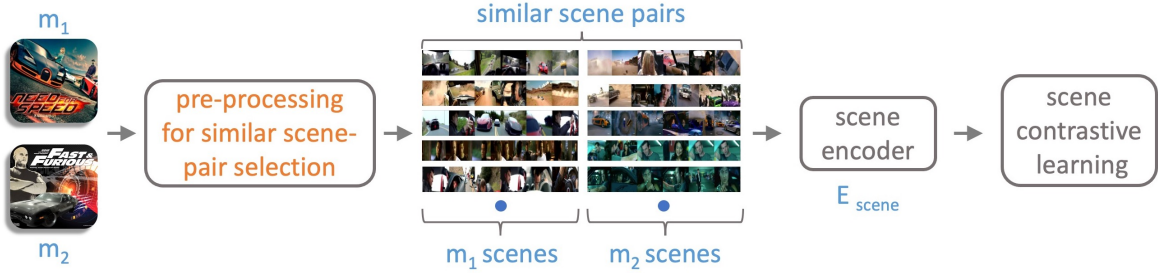


Figure 3: **Contrastive Scene Representation Learning** – Given a pair of similar movies m_1 and m_2 as determined by S , we use a set of pre-processing operations (as identified in Figure 2) to select a set of similar scene-pairs. This process is applied to all pairs of similar movies to get a collection of paired scenes that is used for scene-level contrastive learning.

larity between scenes from similar movies (as defined by S). Second, we use this trained network to select similar scene-pairs for contrastive learning of scene representation. Third, we use the learned scene representation for multiple downstream tasks.

3.1. Movie-Level Similarity Learning

As illustrated in Figure 2, we divide a given movie-pair m_1 and m_2 into their constituent shots [41] x_1 and x_2 respectively. We extract features of these shots using a fixed pre-trained encoder E_{fixed} , so that x_1 and x_2 are represented by two feature matrices $E_{\text{fixed}}(x_1)$ and $E_{\text{fixed}}(x_2)$ respectively. These feature matrices are passed through an encoder with learnable parameters $E_{\text{learnable}}$, followed by their inner-product to create a shot-adjacency matrix A_{x_1, x_2} , *i.e.*:

$$A_{x_1, x_2} = E_{\text{learnable}}(E_{\text{fixed}}(x_1)) \cdot E_{\text{learnable}}(E_{\text{fixed}}(x_2)) \quad (1)$$

Note that entries in A_{x_1, x_2} represent pair-wise similarities between shots in movies m_1 and m_2 .

Using k_a contiguous shots as scenes, we convert the shot-adjacency matrix A_{x_1, x_2} into a scene-adjacency matrix B_{x_1, x_2} by applying average-pooling with kernel size k_a and stride s_a on A_{x_1, x_2} to calculate the average values in each $k_a \times k_a$ window in A_{x_1, x_2} . Furthermore, we apply max-pooling with kernel size k_m and stride s_m on B_{x_1, x_2} followed by flattening the output to get vector V_{x_1, x_2} . Intu-

itively, this step finds the most similar scene-pairs between x_1 and x_2 , where each value in V_{x_1, x_2} represents the highest similarity of scene-pair in a neighborhood of $k_m \times k_m$ scenes in B_{x_1, x_2} . Finally, we learn the projection between V_{x_1, x_2} and the output using layer L_{output} , where our goal is to predict if x_1 and x_2 are similar at movie-level. That is, if x_1 and x_2 are shots from similar movies as defined by S , our target label is 1, and 0 otherwise. During training, we use cross-entropy loss to update $E_{\text{learnable}}$ and L_{output} while E_{fixed} remains unchanged.

A useful way to interpret our movie similarity learning step is to view it from a multiple instance learning (MIL) perspective [5]. The shot-adjacency matrix A_{x_1, x_2} can be considered as a *bag*, while similar scene-pairs can be thought of as positive instances. Unlike some recent MIL-based approaches [1] [17] [33], we simplify our learning process by adopting standard network operations and loss function instead of specially designed ones, which allows us to use existing well-engineered implementations to get better efficiency and scalability in practice.

3.2. Scene Contrastive Learning

Given a similar movie-pair as defined by S , we apply $E_{\text{learnable}}(E_{\text{fixed}}(\cdot))$ to their constituent shots, followed by successive pooling operations to find the scene adjacency matrix B , which is used to select the top 50% similar scene-

pairs. We apply this selection process to all pairs of similar movies to get a collection of paired scenes $\mathbf{P}_{\text{scene}}$ that is used for scene-level contrastive learning. Our contrastive learning approach is shown in Figure 3, and explained below.

3.2.1 Scene Encoder

As the inputs to our encoder $\mathbf{E}_{\text{scene}}$ for scene-contrastive learning are multi-shot sequences, it is important to design $\mathbf{E}_{\text{scene}}$ so that it can effectively model the various relationships among input shots. To this end, we build on recent work of ViT [12], and propose a transformer based $\mathbf{E}_{\text{scene}}$ that treats patches in input shots as tokens.

Specifically, following [12] [38], for a k -frame shot of dimension (k, w, h, c) , we first divide it into a sequence of $(k, \frac{w}{p}, \frac{h}{p}, c)$ patches, where (p, p) is the size of each patch. To input the shot to a transformer with latent vector size of D dimensions, we apply $D \times c$ convolutional kernels with kernel size (p, p) and stride (p, p) to the $(k, \frac{w}{p}, \frac{h}{p}, c)$ patches. This converts the shot into patch embeddings with dimension $(k, D, \frac{w}{p}, \frac{h}{p})$, which is further flattened to a (k, D, N) dimensional tensor where $N = (w \cdot h)/p^2$. Furthermore, we prepend a learnable embedding to the patch embeddings similar to the class token used in [11]. After permutation, the result is $(N + 1, D)$ dimensional patch-embeddings for each of the k frames. We add $(N + 1, D)$ dimensional positional embeddings to patch-embeddings to retain positional information, and pass them to successive multi-headed self-attention (MSA) layers as done in [12].

Similarly, for the input of a scene with n shots, we first divide it into a sequence of $(n \cdot k, \frac{w}{p}, \frac{h}{p}, c)$ patches. After convolution and flattening, we get $(D, N \cdot n \cdot k)$ dimensional patch embeddings. Notice that this is different from the dimension of a frame, and does not match with the dimension of position embeddings. Inspired by [12] where they mentioned that pre-trained position embeddings can be interpolated to fine-tune input of higher resolutions, we propose to generalize this property from frame to shot and scene. That is, we interpolate the N -dimensional position embeddings to $N \cdot n \cdot k$, excluding the 1-dimension corresponding to class token, and add the interpolated position embeddings to patch embeddings before providing them to MSA layers.

This operation offers two **key advantages**:

a. Use of Pre-trained Models: Note that ViT [12] offers impressive performance when trained on large-scale datasets (14M-300M images). Available datasets for long-form video understanding are of significantly smaller scale compared to large-scale image datasets. Our proposed way to apply 2-D interpolation to position embeddings allows us to scale them from single frame to shots and scenes, and enables us to readily adopt powerful models [38] pre-trained on large image datasets for long-form video understanding without explicit temporal modeling as required in [3] [2].

b. Flexibility and Efficiency: Using 2-D interpolation to the position embeddings of our encoder allows it to take variable-length shot-sequences as inputs. This enables our approach to be applicable to the common setting where the lengths of multi-shot sequences in contrastive learning are different from those available in downstream tasks. Moreover, as using 2-D interpolation to position embeddings of our encoder does not add extra computation along the temporal dimension, it allows us to perform training efficiently which is particularly important for large-scale settings.

3.2.2 Contrastive Learning

Our scene-contrastive learning step follows some of the recent works [22] [8] with two key differences: (a) unlike the image or shot-augmentation focused pre-text tasks previously used, we define scene-level pretext task that uses commonly available movie-level information making it more effective for long-form video understanding, and (b) our use of ViT-based [12] scene-encoder allows variable-length inputs and the possibility to adopt large-scale pre-trained models, which is not something that previously used ResNet-based encoders [8] could offer.

Specifically, we define our pretext task as a dictionary look-up for the scenes selected at the end of our movie similarity learning step. That is, given a query scene q , its positive key scene k_0 is determined in $\mathbf{P}_{\text{scene}}$, and the objective is to find k_0 among a set of random scenes $\{k_1, k_2, \dots, k_K\}$. The problem is converted to a $K + 1$ -way classification task by calculating similarity with dot product, and we use InfoNCE as the contrastive loss function [37]:

$$\mathcal{L}_q = -\log \frac{\exp(f(q|\theta_q) \cdot g(k_0|\theta_k)/\tau)}{\sum_{i=0}^K \exp(f(q|\theta_q) \cdot g(k_i|\theta_k)/\tau)} \quad (2)$$

where $f(\cdot|\theta_q)$ is the query encoder with parameters θ_q updated during back-propagation, $g(\cdot|\theta_k)$ is the key encoder with parameters θ_k learned by momentum update as done in [22], and τ is the temperature as illustrated in [51].

During contrastive learning, the scene encoder $\mathbf{E}_{\text{scene}}$ is the query encoder q without the last fully-connected layer, and is updated based on the selected similar scenes $\mathbf{P}_{\text{scene}}$. After training converges, $\mathbf{E}_{\text{scene}}$ is the outcome from this stage, which can then be used for downstream tasks.

3.3 Application to Downstream Tasks

We train encoder $\mathbf{E}_{\text{scene}}$ as detailed above and apply it to downstream tasks as a general-purpose scene-level encoder. Specifically, depending on the downstream task, we first process the video-data to a sequence of shots or frames. Then, we extract features for each sample by $\mathbf{E}_{\text{scene}}$, which then can be used as input for downstream classifiers.

4. Experiments

We first discuss one of our newly collected internal movie datasets MovieCL30K that we used to learn our scene representation followed by describing the implementation details of our algorithm. We then present comparative results on multiple benchmark datasets [50] [25] [39] demonstrating significant gains of our approach over existing state-of-the-art models for **eleven downstream tasks**. To further demonstrate the generalizability of our learned scene-representation, we test it on another newly collected internal dataset MCD focused on large-scale moderation of age-sensitive activities including sex, violence, and drug-use and show substantial gains over existing state-of-the-art models.

4.1. MovieCL30K Dataset

For contrastive learning of our scene-representation, we compiled a new internal dataset called MovieCL30K with 30,340 movies from 11 genres (see Table 1 for genre-distribution). To compute movie-similarity in this data, we used commonly available movie information including: (i) co-watch, (ii) synopsis, and (iii) genre.

Co-watch information is collected based on watch history of movies, similar to the setting of purchase history in recommendation systems [34]. For each movie \mathbf{m}_1 , we keep records of movies that are watched after \mathbf{m}_1 , and then aggregate and rank the records to build a set of movies that are most frequently watched after \mathbf{m}_1 . For each input movie in MovieCL30K, we select its most similar movies based on their co-watch rankings.

To use synopsis for movie-level similarity, we first extract textual-embeddings of movie-synopsis using a pre-trained NLP model [36], and then compute pair-wise movie-similarities as the inner-product of their textual-embeddings followed by selecting the closest movies.

Lastly, to use genre to find movies similar to an input movie, we randomly select movies with the same genre as the input movie. When using any of the aforementioned movie-similarity measures, we select three most similar movies on average for each movie in MovieCL30K.

4.2. Implementation Details

We divide movies in MovieCL30K into their constituent ~ 33 million shots, and only keep one frame per shot for efficiency. Representations of all shots are first extracted using the visual encoder of pre-trained CLIP model [38] denoted as $\mathbf{E}_{\text{fixed}}$ in Figure 2. The encoder $\mathbf{E}_{\text{learnable}}$ comprises of two fully-connected layers each with 512 dimensions, and a dropout layer with 0.5 probability between them. The fact that each movie in MovieCL30K consists more than 1,000 shots on average leads us to keep our $\mathbf{E}_{\text{fixed}}$ constant and to only update parameters of $\mathbf{E}_{\text{learnable}}$ during training to help us achieve high efficiency. We keep length of each movie to

be 1,024 shots, and zero-padded the movies that are shorter than that. Kernel size for both max and average pooling are set to 16×16 , with a stride of 8.

After the completion of movie-level similarity learning (Figure 2), we select the top 50% of most-similar scene-pairs from each movie-pair, and use a scene-length of 9 shots for contrastive learning (Figure 3). We follow the implementation in [22] for momentum contrastive learning and use the ViT [12] from pre-trained CLIP [38] as our scene encoder instead of the ResNet [23]-based encoder used in [22]. Moreover, we optimize with Adam [30] instead of SGD [18]. Unlike movie-level learning where we directly use ViT [12] as a shot-encoder, for scene-representation learning we interpolate the pre-trained position embeddings of ViT [12] (see § 3.2.1) so that the encoder can take variable-length multi-shot sequences as input.

For supervised learning on downstream tasks, unless otherwise specified, we use a simple MLP with two hidden layers, where the output layer is modified based on each of the various classification or regression tasks.

4.3. Comparisons on Benchmark Datasets

To ensure that there is no overlap between pre-training and downstream evaluation, during the representation learning step we exclude movies from MovieCL30K that have the same IMDb IDs as the ones in validation and test sets of benchmark datasets.

4.3.1 4.3.1 – LVU Benchmark

We first compare our model with the state-of-the-art approaches using the benchmark LVU dataset [50] which contains nine diverse tasks including: place (scene), director, relationship, way-of-speaking, writer, year, genre, view-count, and like-ratio. The total number of labeled videos in LVU dataset [50] is 11K with the splits of training, validation and testing sets to be 70%, 15% and 15%, respectively.

a. Effectiveness of Learned Representation: To demonstrate the effectiveness of our learned scene-representation, we use the place-labeled scenes from LVU data [50] in a retrieval-setting. Specifically, using query scenes each with a particular place-label from the validation-set, we retrieve 1, 5 and 10 nearest neighbors from the training-set using their L_2 distances. Precision results for various settings are given in Table 2 where our encoder is compared with the pre-trained visual encoder of CLIP [38] and the SlowFast model [16] pre-trained on Kinetics [6] and AVA [32].

Moreover, to provide qualitative insights into the effectiveness of our learned scene-representation, Figure 4 shows the retrieval results using an example query for 4 of the 6 categories based on ours as well as CLIP [38] visual representation. It can be seen that although CLIP visual representation can capture local appearance-based patterns ef-

Genre	action	drama	comedy	horror	doc	foreign	animation	kids	sci-fi	romance	other
%	27.4	21.6	17.5	6.5	4.6	4.6	4.1	3.1	2.8	1.2	6.1

Table 1: Distribution of movie genres in MovieCL30K dataset.

Models	CLIP [38]			SlowFast [16]			Ours		
Architecture	ViT-B/16 [12]			ResNet-101 [23]			ViT-B/16 [12]		
Pre-training data	400M image-text pairs			Kinetics [6]+AVA [32]			MovieCL30K		
Pre-training task	image-text similarity			action recognition			scene contrast		
	top-1	top-5	top-10	top-1	top-5	top-10	top-1	top-5	top-10
office	30	20	19	0	16	17	40	34	30
airport	0	15	10	0	0	10	0	20	20
school	28.57	26.66	25	76.19	20.47	32.14	45.23	40.95	40.95
hotel	35.71	28.57	29.28	0	0	10	42.85	28.57	26.42
prison	52.94	42.94	42.94	35.29	40	20.29	67.64	44.70	42.94
restaurant	20	13.99	13.99	0	20	10	30	26	19
all queries	35.08	29.64	28.85	38.59	22.63	21.84	48.24	37.89	36.14

Table 2: The place-labeled scenes in LVU data [50] are formulated to a retrieval setting, where the goal is to retrieve similar scenes from training-set given query scenes from validation-set. Representations pre-trained on different configurations as specified in the table are compared. The precision results for different place categories are reported with the size of retrieved set to be 1, 5 and 10.



Figure 4: Qualitative results of place retrieval using LVU data [50] are shown. For each query scene in validation-set, two similar scenes from training-set are retrieved based on ours and CLIP visual representation [38]. Example results show that our feature can capture both scene-appearance as well as their broader thematic signature, while CLIP [38] can only capture scene-appearance effectively.

fectively, it is not able to capture longer-duration semantic aspects of scenes. In contrast, our representation is able to capture the appearance as well as semantic aspects of scenes effectively, and is therefore able to avoid the types of confusions that confound the CLIP representation.

b. Comparative Empirical Analysis: We further compare our approach with state-of-the-art results on LVU [50] test-set quantitatively. Following [50], view-count and like-ratio are evaluated by mean-squared-error in regression (lower is better), while other seven tasks are evaluated using top-1 ac-

curacy in classification (higher is better). Table 3 shows our results compared with SlowFast [16], Video Bert [43], Object Transformer [50] and CLIP visual encoder [38], where our approach comfortably outperforms on all 9 tasks.

Table 3 also shows comparison of our approach with different types of movie-level similarities. It can be seen that genre and synopsis are effective ways to define movie-level similarity, where using genre alone allows us to surpass previous state-of-the-art model [50] on all seven classification tasks. Using co-watch information can achieve

Models	Classification							Regression	
	place	director	relationship	speaking	writer	year	genre	view	like
Video Bert [43]	54.9	47.3	52.8	37.9	38.5	36.1	51.9	4.46	0.320
SlowFast R101 [16]	54.7	44.9	52.4	35.8	36.3	52.5	53	3.77	0.386
Object Transformer [50]	56.9	51.2	53.1	39.4	34.5	39.1	54.6	3.55	0.230
CLIP [38]	52.9	56.2	56.1	36.7	37.8	46.4	50.9	3.85	0.411
Ours (ablation-scale)	53.4	55.2	55.1	36.1	37.7	48.5	50.4	4.03	0.419
Ours (ablation-selection)	57.3	59.3	60.8	39.4	45.5	49.1	51.8	3.72	0.385
Ours (genre)	63.2	57.6	66.8	39.7	47.1	44.8	56	3.86	0.358
Ours (synopsis)	56.4	53.0	65.8	35.7	45.4	35.1	49.7	3.88	0.471
Ours (genre+synopsis)	66.3	65.2	69.7	42.6	51.5	51.8	56.6	2.97	0.204
Ours (co-watch)	63.8	65.1	67.7	44.9	56.2	54.7	57.5	2.46	0.153

Table 3: Quantitative comparisons on test-set of benchmark LVU dataset [50]. Our approach is evaluated on nine diverse tasks and compared against multiple state-of-the-art models. Comparisons of our approach using different movie-level similarities are also provided. Note that for classification tasks higher is better, whereas for regression tasks lower is better.

even better results, which is likely due to the fact that it can incorporate more complex relationships between movies, which can provide more diverse scene-pairs during representation learning. Moreover, since genre and synopsis are both metadata-based information, we concatenate the features learned by them (genre+synopsis) and show that it offers similar or even better accuracy compared to co-watch, which indicates that further improvements can be achieved when combining scene-representations learned from different movie similarities obtained using different types of metadata information.

4.3.2 4.3.2 – MovieNet Benchmark

MovieNet is a large-scale movie understanding dataset with 1,100 movies covering a variety of tasks [25]. However, unlike LVU [50] where videos are publicly available, the movies in MovieNet are not publicly released yet due to copyright issues. Only keyframes from each shot are provided, which makes tasks that demand high frame-rate (*e.g.*, action recognition) infeasible. We therefore focus our comparison to two scene understanding related tasks in MovieNet that do not demand particularly high frame-rate, *i.e.*: (i) place-tagging, and (ii) scene-boundary-detection. The key difference between these two tasks is that place-tagging focuses more on the holistic understanding of the scene, while scene-boundary-detection requires the understanding of the relationships among multiple-shots. Our results demonstrate that our scene-representation can work well under both these settings and surpasses their existing state-of-the-art approaches.

a. Place Tagging: The MovieNet [25] dataset contains 90 categories of places with 19.6K place tags. The place-tagging problem is formulated as a multi-label classification task where each manually-labeled scene can have multiple place-tags. The results are evaluated by mean average precision (mAP) on the test-set as shown in Table 4. We compare

Models		mAP
Fine-tuning	TSN [47]	8.33
	I3D [7]	7.66
Feature+MLP	ImageNet [10]	7.04
	Place [54]	8.76
	CLIP [38]	9.26
	Ours	12.13

Table 4: Comparisons with state-of-the-art results on MovieNet place scene tagging using methods based on: (a) action recognition models fine-tuned for this task, and (b) commonly used pre-trained representations for generic downstream tasks.

Models	Pre-training setting	AP
SimCLR [9]	same-domain	41.65
MoCo [22]	same-domain	42.51
ShotCoL [8]	same-domain	53.37
LGSS [39]	cross-domain	47.1
CLIP [38]	cross-domain	47.4
ShotCoL [8]	cross-domain	48.4
Ours	cross-domain	54.22

Table 5: Comparisons with state-of-the-art results on scene boundary detection, showing that our approach outperforms state-of-the-art even when pre-trained in cross-domain setting.

our approach with two sets of models: (i) fine-tuning models, and (ii) feature-based approaches. The results on fine-tuning are reported by [25] where they mentioned that standard action recognition models were adopted. For feature-based approaches, we compare our encoder with CLIP visual encoder [38] and ResNet50 [23] pre-trained on the Place dataset [54]. We can see that our model can significantly outperform all other compared methods on the place-tagging task in MovieNet [25] data.

b. Scene Boundary Detection: Scene-boundary-detection (SBD) is a challenging and important problem for semantic movie understanding [39][8]. Unlike previous approaches

that proposed dedicated SBD models, we show that our learned general-purpose scene encoder can be seamlessly applied to this task and outperform state-of-the-art SBD results. Following [8], we use the subset of 318 movies from MovieNet [39][25] where manually annotated scene boundaries are provided. The training, testing and validation splits are also provided with 190, 64 and 64 movies respectively. The problem is formulated as a binary classification problem to predict if a shot boundary is also a scene boundary, and the results are evaluated by average precision (AP) [25][8]. Following ShotCoL [8], we use a four-shot sequence as a sample where representations for each shot are independently extracted and concatenated.

We report the AP results of the different compared approaches in Table 5. Notice that all compared methods include two components, *i.e.*, an encoder and a predictor. However, the encoder-settings for different approaches are different depending on whether the pre-training data comes from the same domain as the downstream task. For example, there are four pre-trained encoders in LGSS [39] with features related to visual, audio, action and actor, respectively. These encoders were pre-trained in a supervised manner on datasets that are different from MovieNet [25], and thus it is the cross-domain setting. For MoCo [22] implemented in [8], the representations were learned on the full MovieNet [25] dataset with 1,100 movies by the pretext task of image augmentation, and then applied to the subset of 318 movies on SBD, making it a same-domain setting. ShotCoL [8] provided results for both settings with a significant performance gap between them. This indicates that even with same pretext task, performance on downstream tasks can vary significantly if domain discrepancy exists.

Importantly, our approach outperforms state-of-the-art results even when used in cross-domain setting. Also, notice that our scene encoder can conveniently take a single shot as input and provide effective representation, which further validates the flexibility and generalizability of our approach. Recall that we have 2.5 million pairs of samples for contrastive learning, while ShotCoL [8] had 1.5 million and 2.2 million pairs for same-domain and cross-domain settings respectively. This shows that we have comparable data-scale as previous works during contrastive learning.

4.3.3 4.3.3 – Ablation Studies

To identify the influence of different components in our approach, we present ablative results regarding three factors during pre-training.

a. Pre-Training Data Scale: Pre-training data scale is an important factor that can impact the accuracy on downstream tasks. This point is further distilled by the row Ours (ablation-scale) in Table 3 which shows results of pre-training based on co-watch of 10K movies in

MovieCL30K with 900K scene-pairs. As also noted by previous works[38][9], our results show that data scale can substantially influence effectiveness of representation learning.

b. Scene-Pair Selection: We show in Table 3 a comparison of using different feature spaces for scene-pair selection. Specifically, the row Ours (ablation-selection) uses pretrained CLIP visual features [38] (as opposed to using a learnable encoder) to select similar scenes from given movie-pairs defined using co-watch information. In contrast, the row Ours (co-watch) uses the feature space of our learnable encoder for similar scene selection. Lastly, row CLIP directly uses CLIP features [38] without incorporating any further contrastive learning. We see that Ours (ablation-selection) offers better accuracy than simply using baseline CLIP. However, the results of Ours (ablation-selection) are not competitive with Ours (co-watch) which signifies the importance of learning of feature space based on movie-level similarity.

c. Number of Frames and Shots: Number of keyframes and number of shots used can substantially influence model performance. As more information can be captured using more shots and frames, it can generally help improve the performance on certain downstream tasks [8]. In our experiments, we achieved an mAP of 12.13 in Table 4 for MovieNet place scene tagging task when using 9 shots, while using 4 shots resulted in 9.37 mAP. For this work, we empirically choose 9 shots with 1 frame per shot based on factors such as our achieved accuracy, computational efficiency, and the scale of pre-training dataset.

4.4. Video Moderation

To further demonstrate the generalizability of our scene-representation, we focus on video-moderation particularly to detect sex, violence, and drug-use activities in movies and TV shows. Video-moderation is one of the most pressing challenges faced by all video-streaming services. However, most of the existing activity datasets (*e.g.*, Kinetics [29, 6], Thumos14 [27]) do not focus on movies and TV series. Also, existing movie datasets (AVA [20], MovieNet [25]) do not focus on detecting age-appropriate activities. In the following, we first go over a new internal data for large-scale video-moderation in studio-produced content, followed by presenting comparative results using this data.

a. Mature Content Dataset (MCD): Our dataset focuses on three age-appropriate activities, *i.e.*: (a) sex, (b) violence, and (c) drug-use (see Figure 5 for examples). We used Amazon SageMaker Ground Truth as our labeling tool. To have consistent and reliable annotations among data-annotators, we provided annotation guidelines to them consisting of 17 instructions for sex, 34 for violence and 14 for drug-use. Examples of these instructions include: “intentional murder and/or suicide that involves bloody injury”



Figure 5: Examples of 3 types of age-appropriate activities in our data. Sensitive parts of images have been intentionally redacted here.

Models	Pre-training data	sex	violence	drug-use	average
SlowFast R50 [16]	K400 [29]	63.9	46.5	49.4	53.3
SlowFast R101 [16]	K600 [6]+AVA2.2 [32]	61.0	57.3	54.0	57.4
X3D-L [15]	K400 [29]	69.2	49.4	56.4	58.4
CLIP [38]	400M image-text pairs	78.5	62.1	55.1	65.2
Ours	MovieCL30K	81.8	70.1	62.2	71.3

Table 6: Comparisons of our approach with state-of-the-art action recognition models and CLIP visual encoder [38] on MCD dataset.

for violence, and “strip-tease or erotic dancing with full nudity” for sex.

All our annotators were fluent English speakers which enabled them to understand their provided instructions. All annotators went through multiple training sessions to prepare for their assignment. Each annotator was asked to label sample-videos and received feedback on their labeling quality before they could start to label data independently. Additionally, 20% of labeled samples were randomly selected and taken through a mandatory review to ensure quality.

Our data contains 44,581 clips from 18,330 movies and TV episodes with 4,580, 8,248, 8,271, and 23,482 clips containing sex, violence, drug-use, and none-of-the-above activities respectively. These clips have a mean duration of 5 seconds, and were divided into training, validation, and testing sets with 70%, 10%, and 20% ratio respectively.

b. Results: We extract embeddings of our mature-content dataset using our pre-trained scene encoder and use them as input to train a 4-class MLP model for predicting age-appropriate activities. We compare our representation with the representations learned using state-of-the-art models on existing action recognition as well as image classification datasets. To this end, we apply action recognition models [16] [14] [15] trained on Kinetics [29, 6] and AVA [20] as well as CLIP visual encoder [38] on clips in our dataset, extract the embeddings from these models, and provide them as inputs to the aforementioned MLP model for training. Table 6 presents the AP results on our test data, and shows that our scene representation outperforms the alterna-

tives by a large margin. Notice that CLIP visual feature performed close to our representation on the task of sex but not other tasks. This might indicate that in the pre-training data of CLIP, there might be a considerable amount of image-text pairs related to sex concepts. Similar observations [4] have been made on other large scale datasets [40].

5. Conclusions

We presented a novel contrastive learning approach that uses movie-level similarity to learn a general-purpose scene-level representation. Our approach adopts recent developments in vision transformer, where by incorporating the interpolation of pre-trained position-embedding, we were able to train a scene-encoder that can take variable-length multi-shot inputs. We empirically validated that our approach works effectively with different types of movie-level similarities including genre, synopsis and co-watch information. Qualitative and quantitative results on diverse tasks from multiple benchmark datasets highlight the strengths of our approach. We also presented a new application of our scene-representation for video moderation focused on three age-appropriate activities, where our approach outperformed state-of-the-art action recognition features. Going forward, we plan to further improve the computational efficiency of our approach to help it scale even more. We will also explore other types of commonly available movie-level information to find a representation that is effective on additional tasks including action recognition and image classification.

References

[1] Baptiste Angles, Yuhe Jin, Simon Kornblith, Andrea Tagliasacchi, and Kwang Moo Yi. Mist: Multiple instance spatial transformer. In *CVPR*, 2021. 3

[2] Anurag Arnab, Mostafa Dehghani, Georg Heigold, Chen Sun, Mario Lučić, and Cordelia Schmid. Vivit: A video vision transformer. *arXiv:2103.15691*, 2021. 2, 4

[3] Gedas Bertasius, Heng Wang, and Lorenzo Torresani. Is space-time attention all you need for video understanding? *arXiv:2102.05095*, 2021. 2, 4

[4] Abeba Birhane, Vinay Uday Prabhu, and Emmanuel Kahembwe. Multimodal datasets: misogyny, pornography, and malignant stereotypes. *arXiv:2110.01963*, 2021. 9

[5] Marc-André Carbonneau, Veronika Cheplygina, Eric Granger, and Ghyslain Gagnon. Multiple instance learning: A survey of problem characteristics and applications. *Pattern Recognition*, 2018. 3

[6] Joao Carreira, Eric Noland, Andras Banki-Horvath, Chloe Hillier, and Andrew Zisserman. A short note about kinetics-600. *arXiv:1808.01340*, 2018. 5, 6, 8, 9

[7] Joao Carreira and Andrew Zisserman. Quo vadis, action recognition? a new model and the kinetics dataset. In *CVPR*, 2017. 2, 7

[8] Shixing Chen, Xiaohan Nie, David Fan, Dongqing Zhang, Vimal Bhat, and Raffay Hamid. Shot contrastive self-supervised learning for scene boundary detection. In *CVPR*, 2021. 1, 2, 4, 7, 8

[9] Ting Chen, Simon Kornblith, Mohammad Norouzi, and Geoffrey Hinton. A simple framework for contrastive learning of visual representations. In *ICML*, 2020. 1, 2, 7, 8

[10] Jia Deng, Wei Dong, Richard Socher, Li-Jia Li, Kai Li, and Li Fei-Fei. Imagenet: A large-scale hierarchical image database. In *CVPR*, 2009. 7

[11] Jacob Devlin, Ming-Wei Chang, Kenton Lee, and Kristina Toutanova. Bert: Pre-training of deep bidirectional transformers for language understanding. *arXiv:1810.04805*, 2018. 2, 4

[12] Alexey Dosovitskiy, Lucas Beyer, Alexander Kolesnikov, Dirk Weissenborn, Xiaohua Zhai, Thomas Unterthiner, Mostafa Dehghani, Matthias Minderer, Georg Heigold, Sylvain Gelly, Jakob Uszkoreit, and Neil Houlsby. An image is worth 16x16 words: Transformers for image recognition at scale. *ICLR*, 2021. 1, 2, 4, 5, 6

[13] Debidatta Dwibedi, Yusuf Aytar, Jonathan Tompson, Pierre Sermanet, and Andrew Zisserman. With a little help from my friends: Nearest-neighbor contrastive learning of visual representations. In *ICCV*, 2021. 1

[14] Haoqi Fan, Bo Xiong, Karttikeya Mangalam, Yanghao Li, Zhicheng Yan, Jitendra Malik, and Christoph Feichtenhofer. Multiscale vision transformers. In *ICCV*, 2021. 2, 9

[15] Christoph Feichtenhofer. X3d: Expanding architectures for efficient video recognition. In *CVPR*, 2020. 9

[16] Christoph Feichtenhofer, Haoqi Fan, Jitendra Malik, and Kaiming He. Slowfast networks for video recognition. In *ICCV*, 2019. 2, 5, 6, 7, 9

[17] Jia-Chang Feng, Fa-Ting Hong, and Wei-Shi Zheng. Mist: Multiple instance self-training framework for video anomaly detection. In *CVPR*, 2021. 3

[18] Priya Goyal, Piotr Dollár, Ross Girshick, Pieter Noordhuis, Lukasz Wesolowski, Aapo Kyrola, Andrew Tulloch, Yangqing Jia, and Kaiming He. Accurate, large minibatch sgd: Training imagenet in 1 hour. *arXiv:1706.02677*, 2017. 5

[19] Jean-Bastien Grill, Florian Strub, Florent Altché, Corentin Tallec, Pierre H Richemond, Elena Buchatskaya, Carl Doersch, Bernardo Avila Pires, Zhaohan Daniel Guo, Mohammad Gheshlaghi Azar, et al. Bootstrap your own latent: A new approach to self-supervised learning. *arXiv:2006.07733*, 2020. 2

[20] Chunhui Gu, Chen Sun, David A Ross, Carl Vondrick, Caroline Pantofaru, Yeqing Li, Sudheendra Vijayanarasimhan, George Toderici, Susanna Ricco, Rahul Sukthankar, et al. Ava: A video dataset of spatio-temporally localized atomic visual actions. In *CVPR*, 2018. 8, 9

[21] Tengda Han, Weidi Xie, and Andrew Zisserman. Memory-augmented dense predictive coding for video representation learning. In *ECCV*, 2020. 2

[22] Kaiming He, Haoqi Fan, Yuxin Wu, Saining Xie, and Ross Girshick. Momentum contrast for unsupervised visual representation learning. In *CVPR*, 2020. 1, 2, 4, 5, 7, 8

[23] Kaiming He, Xiangyu Zhang, Shaoqing Ren, and Jian Sun. Deep residual learning for image recognition. In *CVPR*, 2016. 5, 6, 7

[24] Olivier J Henaff, Aravind Srinivas, Jeffrey De Fauw, Ali Razavi, Carl Doersch, S. M. Ali Eslami, and Aaron van den Oord. Data-efficient image recognition with contrastive predictive coding. In *ICML*, 2020. 2

[25] Qingqiu Huang, Yu Xiong, Anyi Rao, Jiaze Wang, and Dahua Lin. Movienet: A holistic dataset for movie understanding. In *ECCV*, 2020. 1, 2, 5, 7, 8

[26] Ashish Jaiswal, Ashwin Ramesh Babu, Mohammad Zaki Zadeh, Debapriya Banerjee, and Fillia Makedon. A survey on contrastive self-supervised learning. *Technologies*, 2021. 1

[27] Y.-G. Jiang, J. Liu, A. Roshan Zamir, G. Toderici, I. Laptev, M. Shah, and R. Sukthankar. THUMOS challenge: Action recognition with a large number of classes. <http://crcv.ucf.edu/THUMOS14/>, 2014. 2, 8

[28] Longlong Jing and Yingli Tian. Self-supervised visual feature learning with deep neural networks: A survey. *TPAMI*, 2020. 2

[29] Will Kay, Joao Carreira, Karen Simonyan, Brian Zhang, Chloe Hillier, Sudheendra Vijayanarasimhan, Fabio Viola, Tim Green, Trevor Back, Paul Natsev, et al. The kinetics human action video dataset. *arXiv:1705.06950*, 2017. 8, 9

[30] Diederik P Kingma and Jimmy Ba. Adam: A method for stochastic optimization. *arXiv:1412.6980*, 2014. 5

[31] Phuc H Le-Khac, Graham Healy, and Alan F Smeaton. Contrastive representation learning: A framework and review. *IEEE Access*, 2020. 2

[32] Ang Li, Meghana Thotakuri, David A Ross, João Carreira, Alexander Vostrikov, and Andrew Zisserman.

The ava-kinetics localized human actions video dataset. *arXiv:2005.00214*, 2020. 5, 6, 9

[33] Bin Li, Yin Li, and Kevin W. Eliceiri. Dual-stream multiple instance learning network for whole slide image classification with self-supervised contrastive learning. In *CVPR*, 2021. 3

[34] Greg Linden, Brent Smith, and Jeremy York. Amazon.com recommendations: Item-to-item collaborative filtering. *IEEE Internet Computing*, 2003. 5

[35] Xiaolong Liu, Yao Hu, Song Bai, Fei Ding, Xiang Bai, and Philip H. S. Torr. Multi-shot temporal event localization: A benchmark. In *CVPR*, 2021. 2

[36] Yinhan Liu, Myle Ott, Naman Goyal, Jingfei Du, Mandar Joshi, Danqi Chen, Omer Levy, Mike Lewis, Luke Zettlemoyer, and Veselin Stoyanov. Roberta: A robustly optimized bert pretraining approach. *arXiv:1907.11692*, 2019. 5

[37] Aaron van den Oord, Yazhe Li, and Oriol Vinyals. Representation learning with contrastive predictive coding. *arXiv:1807.03748*, 2018. 4

[38] Alec Radford, Jong Wook Kim, Chris Hallacy, Aditya Ramesh, Gabriel Goh, Sandhini Agarwal, Girish Sastry, Amanda Askell, Pamela Mishkin, Jack Clark, et al. Learning transferable visual models from natural language supervision. *arXiv:2103.00020*, 2021. 1, 2, 4, 5, 6, 7, 8, 9

[39] Anyi Rao, Linning Xu, Yu Xiong, Guodong Xu, Qingqiu Huang, Bolei Zhou, and Dahua Lin. A local-to-global approach to multi-modal movie scene segmentation. In *CVPR*, 2020. 1, 2, 5, 7, 8

[40] Christoph Schuhmann, Richard Vencu, Romain Beaumont, Robert Kaczmarczyk, Clayton Mullis, Aarush Katta, Theo Coombes, Jenia Jitsev, and Aran Komatsuzaki. Laion-400m: Open dataset of clip-filtered 400 million image-text pairs. *arXiv:2111.02114*, 2021. 9

[41] Panagiotis Sidiropoulos, Vasileios Mezaris, Ioannis Kompatiari, Hugo Meinedo, Miguel Bugalho, and Isabel Trancoso. Temporal video segmentation to scenes using high-level audiovisual features. *IEEE Transactions on Circuits and Systems for Video Technology*, 2011. 3

[42] Robert Sklar. Film: An international history of the medium. *Thames and Hudson*, 1990. 2

[43] Chen Sun, Austin Myers, Carl Vondrick, Kevin Murphy, and Cordelia Schmid. Videobert: A joint model for video and language representation learning. In *ICCV*, 2019. 2, 6, 7

[44] Yonglong Tian, Chen Sun, Ben Poole, Dilip Krishnan, Cordelia Schmid, and Phillip Isola. What makes for good views for contrastive learning? *arXiv:2005.10243*, 2020. 2

[45] Hugo Touvron, Matthieu Cord, Matthijs Douze, Francisco Massa, Alexandre Sablayrolles, and Hervé Jégou. Training data-efficient image transformers & distillation through attention. In *ICML*, 2021. 2

[46] Ashish Vaswani, Noam Shazeer, Niki Parmar, Jakob Uszkoreit, Llion Jones, Aidan N Gomez, Łukasz Kaiser, and Illia Polosukhin. Attention is all you need. In *NeurIPS*, 2017. 2

[47] Limin Wang, Yuanjun Xiong, Zhe Wang, Yu Qiao, Dahua Lin, Xiaoou Tang, and Luc Van Gool. Temporal segment networks: Towards good practices for deep action recognition. In *ECCV*, 2016. 7

[48] Yaqing Wang, Quanming Yao, James T Kwok, and Lionel M Ni. Generalizing from a few examples: A survey on few-shot learning. *ACM Computing Surveys*, 2020. 1

[49] Thomas Wolf, Julien Chaumond, Lysandre Debut, Victor Sanh, Clement Delangue, Anthony Moi, Pierrick Cistac, Morgan Funtowicz, Joe Davison, Sam Shleifer, et al. Transformers: State-of-the-art natural language processing. In *Conference on Empirical Methods in Natural Language Processing: System Demonstrations*, 2020. 2

[50] Chao-Yuan Wu and Philipp Krahenbuhl. Towards long-form video understanding. In *CVPR*, 2021. 1, 2, 5, 6, 7

[51] Zhirong Wu, Yuanjun Xiong, X Yu Stella, and Dahua Lin. Unsupervised feature learning via non-parametric instance discrimination. In *CVPR*, 2018. 4

[52] Mengmeng Xu, Chen Zhao, David S Rojas, Ali Thabet, and Bernard Ghanem. G-tad: Sub-graph localization for temporal action detection. In *CVPR*, 2020. 2

[53] Runhao Zeng, Wenbing Huang, Mingkui Tan, Yu Rong, Peilin Zhao, Junzhou Huang, and Chuang Gan. Graph convolutional networks for temporal action localization. In *ICCV*, 2019. 2

[54] Bolei Zhou, Agata Lapedriza, Aditya Khosla, Aude Oliva, and Antonio Torralba. Places: A 10 million image database for scene recognition. *TPAMI*, 2017. 7

[55] Mohammadreza Zolfaghari, Yi Zhu, Peter Gehler, and Thomas Brox. Crossclr: Cross-modal contrastive learning for multi-modal video representations. In *ICCV*, 2021. 2

Supplementary Material

Movies2Scenes: Learning Scene Representations Using Movie Similarities

Shixing Chen Xiang Hao Xiaohan Nie Raffay Hamid
Amazon Prime Video

{shixic, xianghao, nxiaohan, raffay}@amazon.com

In this supplementary material, we provide two sections to better support the arguments and results in the main paper: (a) more details of the specific settings in our experiments for better reproducibility, and (b) more extensive qualitative results to better demonstrate the interpretability of our learned representations. The sections will be presented with information corresponding to different datasets used in the main paper including: Movie Contrastive Learning 30K (MovieCL30K) dataset, Long-Form Video Understanding (LVU) dataset [11], MovieNet dataset [6] [10] and Mature Content Dataset (MCD).

1. Experiment Details

We use PyTorch [8] as our deep learning library and Tesla V100 GPUs for computation. During contrastive learning, we use 8 GPUs with distributed data parallelism. For supervised learning of MLP on downstream tasks, only 1 GPU is needed.

1.1. MovieCL30K

This section corresponds to §4.2 in the main paper.

a. Movie-Level Similarity Learning: When using movie-level information to train the learnable parameters (Figure 2 in the main paper) on MovieCL30K, we used SGD to optimize with learning rate of 0.1, batch size of 256 and epoch number of 20. The same set of hyper-parameters was applied to all three types of movie-level information (more-like-this, genre and synopsis). Recall that within each batch, there are 256 pairs of movies represented by feature matrices extracted from fixed pre-trained visual encoder in CLIP [9], and the dimension of each feature matrix is 1024×512 . These pairs are passed through $\mathbf{E}_{\text{learnable}}$ to predict whether two movies are similar based on movie-level information.

b. Scene Contrastive Learning: After movie-level similarity learning, we select the set of similar scene-pairs based on the learned space in $\mathbf{E}_{\text{learnable}}$. Specifically, after extracting the CLIP visual feature [9] of all shots in each input movie, the movie is represented as a matrix of $M \times 512$,

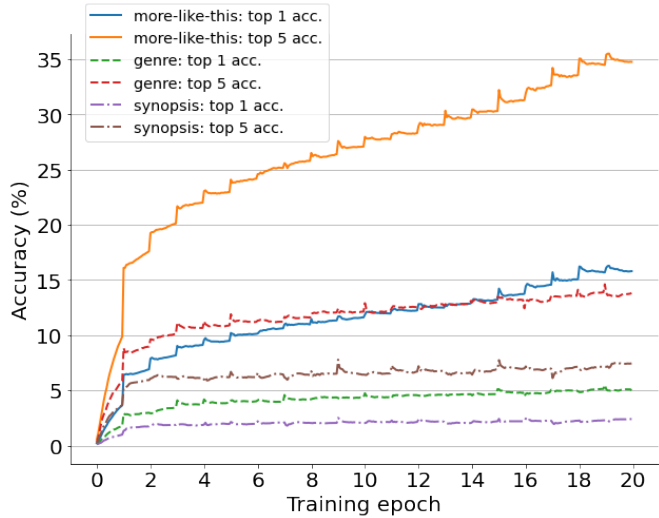


Figure 1: During pre-training on different movie-level information, top-1 and top-5 accuracy results are presented. By using more-like-this information, the accuracy is higher than other information. This may indicate that the representations learned on more-like-this are more discriminating, which leads to better performance on downstream tasks shown in Table 2 of the main paper.

where M is the number of shots in the movie. Notice that the length of the movie is no longer restricted to 1024, so that all shots can be considered during similar scene selection. The feature matrix is then passed to $\mathbf{E}_{\text{learnable}}$ before the last fully-connected layer, and becomes a new feature matrix. Similar process is done on another movie considered similar to the input movie with N shots, and the shot adjacency matrix \mathbf{A} of these two movies takes the size of $M \times N$. We then go through all 9×9 windows in \mathbf{A} with stride 1, and calculate the average value in each window to represent the scene-level similarity of the two movies. Finally, we pop the scene-pairs with top 50% highest scene-level similarity scores while keeping the selected scenes to be non-overlapping in each movie. This generates a set of scene-pairs for each type of movie-level information.

Models	Classification							Regression	
	place	director	relationship	speaking	writer	year	genre	view	like
learning rate	0.1	0.1	0.5	0.01	0.1	0.1	0.01	0.01	0.1
batch size	64	16	16	32	16	64	128	16	16
epoch	400	400	400	400	400	400	400	500	500
drop out	0.25	0.875	0.25	0.75	0.75	0.75	0.25	0.75	0.5

Table 1: Hyper-parameters used in the MLPs for LVU tasks.

With the generated set of scene pairs, we use them for scene contrastive learning following the MoCo framework, while substituting encoder to be ViT [1] in pre-trained CLIP [9] and optimization to be Adam [7] instead of SGD [4]. Specifically, following [5], we use feature dimension of 128, queue size of 65,536, MoCo momentum of 0.999 and softmax temperature of 0.07 during momentum contrastive learning. Following [1][9], we use learning rate of $5e-6$, weight decay of $1e-8$, number of warm-up epochs of 5, batch size of 128 and number of epoch of 20.

We present the top-1 and top-5 accuracy during pre-training on different movie-level information (more-like-this, genre and synopsis) in Figure 1. We can see that more-like-this information gets the highest top-1 and top-5 accuracy during pre-training, while synopsis gets the lowest ones, which indicates that more discriminating features have been learned from more-like-this information leading to give better performance on downstream tasks validated in Table 2 in the main paper. Also notice that the accuracy at the beginning of each epoch is less stable therefore producing the peaks in Figure 1.

1.2. LVU

This section corresponds to §4.3.1 in the main paper.

a. Effectiveness of Learned Representation: We presented the results in Table 1 and Figure 5 in the main paper based on a single model of our approach pre-trained on more-like-this information. In Table 1, when comparing with CLIP feature [9], we adopted the visual encoder from pre-trained CLIP, and extracted features for each shot in the input scene, followed by average pooling. The rationale of average pooling instead of concatenation is that, during retrieval, we do not want the order of shots to influence the results, thus, having one vector per input scene is reasonable. Notice that for the place of airport, both our representation and CLIP have top-1 accuracy of 0 in Table 1 in the main paper, it is because the number of query is very limited in the validation set of LVU [11] (4 airport-labeled scenes), and thus the airport example presented in Figure 5 in the main paper comes from the top-2 retrieval result.

b. Comparative Empirical Analysis: When producing the results in Table 2 in the main paper, following [11] where the model of each task is trained separately with parameters selected by validation set, we selected the parameters and hyper-parameters of MLP for each task by the validation

set in LVU and presented corresponding results on test set. The hyper-parameters used in MLPs of each task on representations pre-trained by more-like-this is shown in Table 1.

1.3. MovieNet

This section corresponds to §4.3.2 in the main paper.

a. Place Tagging: For the results of Ours in Table 3 in the main paper, we used MLP with two 512-dimensional hidden layers optimized by SGD with leaning rate of 5.0, drop out of 0.25, epoch number of 200 and batch size of 512. The problem was formulated as a multi-label classification task and optimized by BCEWithLogitsLoss [8].

b. Scene Boundary Detection: For the results of Ours in Table 4 in the main paper, we used MLP with two 512-dimensional hidden layers optimized by SGD with leaning rate of 0.03, drop out of 0.8, epoch number of 800 and batch size of 4096.

1.4. MCD

We used SlowFast 8x8 R50 and SlowFast 8x8 R101 for the SlowFast models [3] used in Table 5 in the main paper. Both models take 64 frames from each video clips. When extracting representation from the SlowFast models, we used the average pooling layers before the final classification layer, and the representation has 2304 dimensions concatenated from the slow and fast pathways. Similarly for the X3D-L model [2], we used the fully connected layer before the final classification layer, which has 2048 dimensions, and the X3D-L model takes 16 frames from each video clips. For the CLIP model [9], we used ViT-B/16 based visual encoder, and it takes the same 9 frames as the input to our model from each video clip. We first extracted the embeddings with 512 dimensions from each frame and then do an average pooling across all 9 frames, which is used as the representation for the CLIP model. For training the model to classify the age-appropriate activities, we used a 3-layer MLP model with 512 nodes in the intermediate layers.

2. Qualitative Results

2.1. MovieCL30K

We present the similar scene pairs selected by our scene representation learned on more-like-this in Figure 2. We also present the similar scene-pairs found by pre-trained CLIP

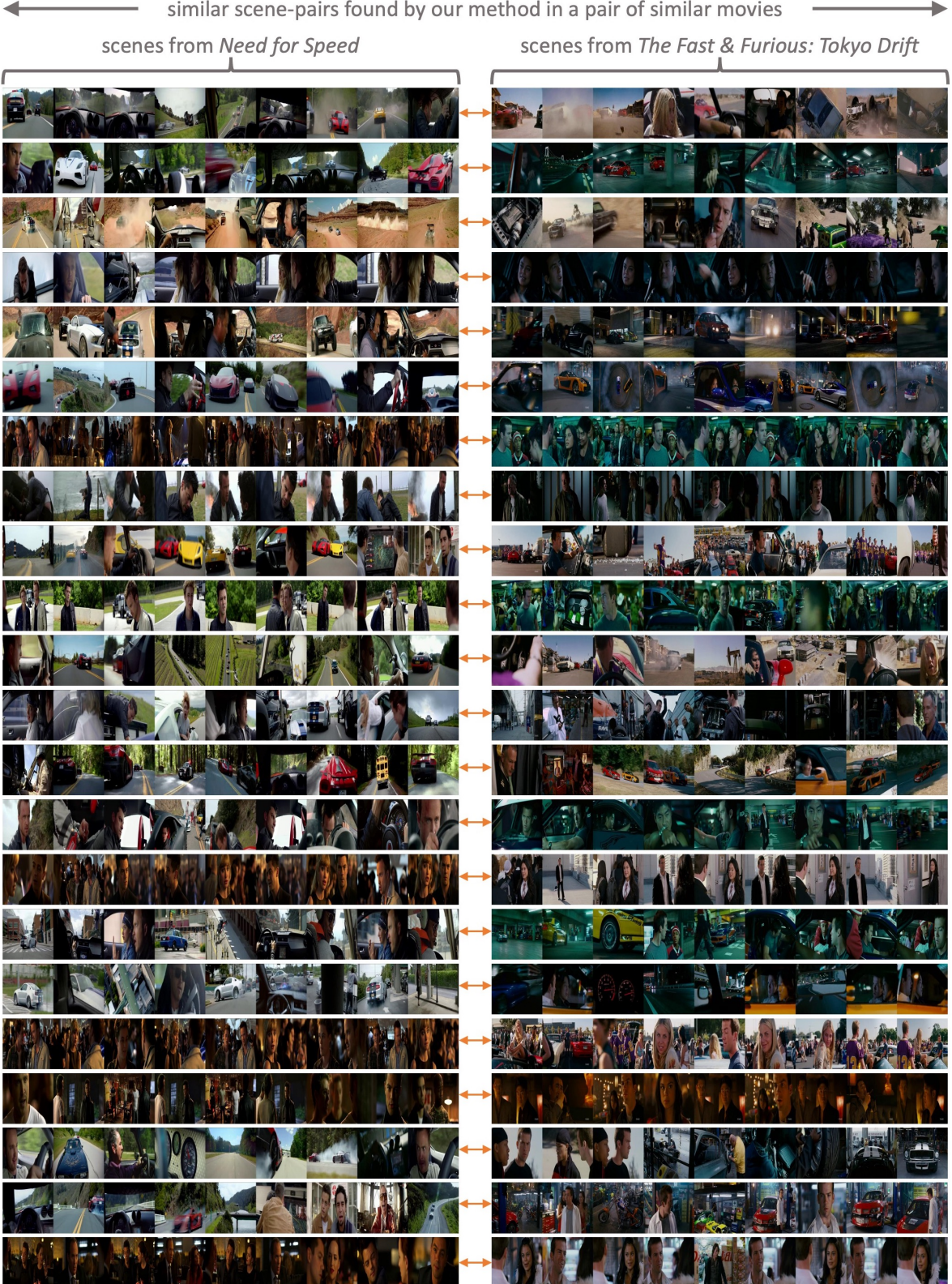


Figure 2: Similar scene-pairs found by our representation - Given a similar movie-pair *Need For Speed* and *The Fast & Furious: Tokyo Drift*, we present representative examples from the set of similar scene-pairs (connected by orange arrow) found by our representation (sorted by similarity). Comparing with the ones found by CLIP visual feature [9] in Figure 3, these scene-pairs are more thematically meaningful, which contributes to the effectiveness of our representation on downstream tasks related to semantic scene understanding.

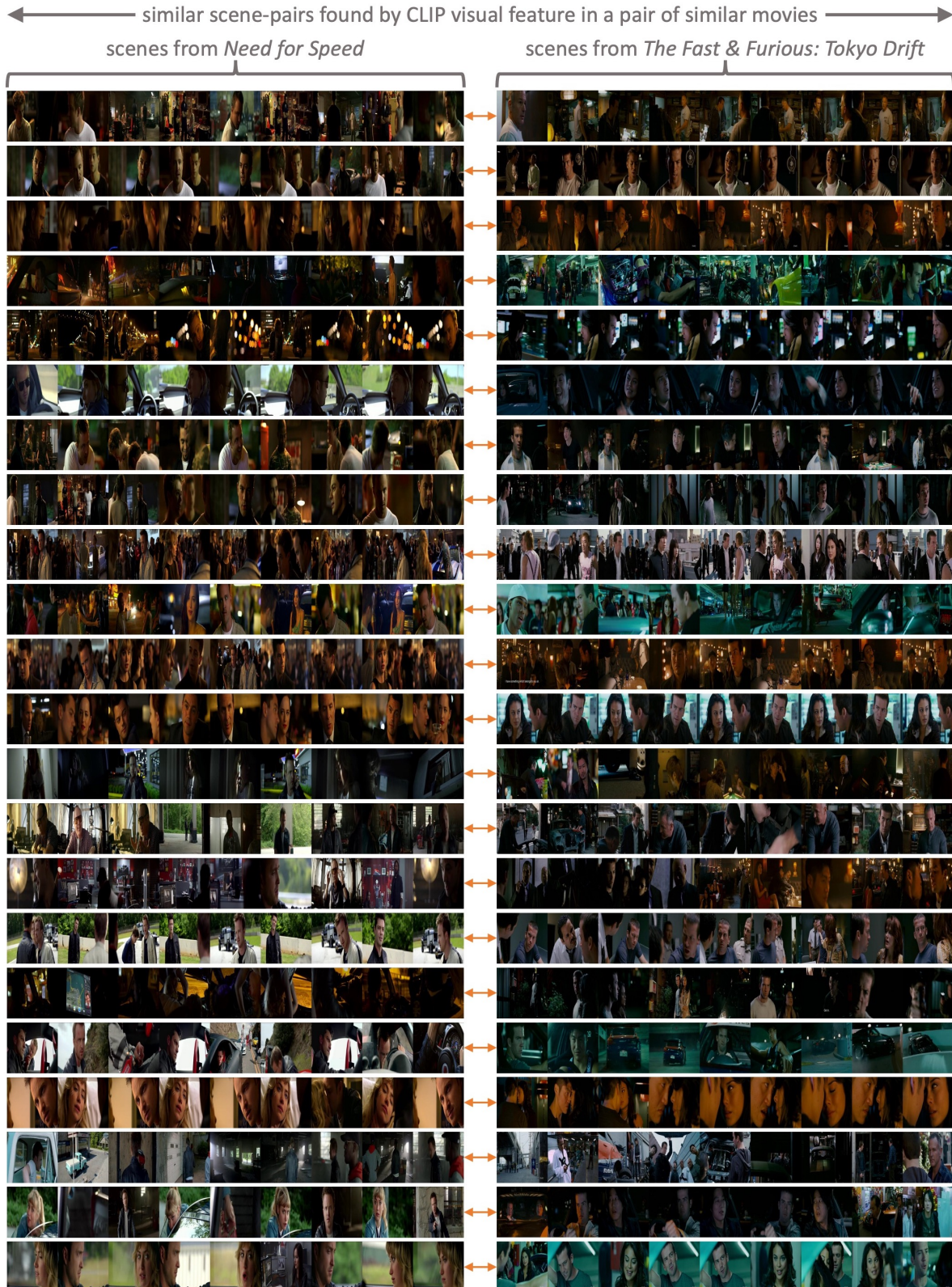


Figure 3: Similar scene-pairs found by CLIP - Given a similar movie-pair *Need For Speed* and *The Fast & Furious: Tokyo Drift*, we present representative examples from the set of similar scene-pairs (connected by orange arrow) found by CLIP visual feature [9] (sorted by similarity). Comparing with the ones found by our representation in Figure 2, these scene-pairs focus more on appearance-based similarity and are mostly related to human faces, which are not sufficiently semantically meaningful for semantic scene understanding.

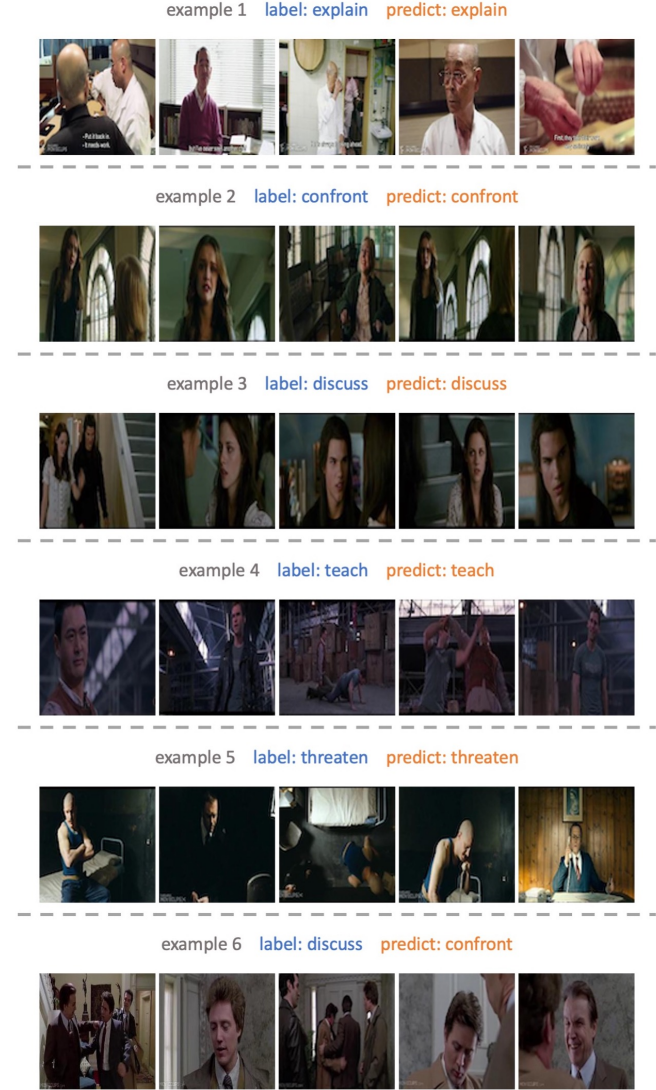


Figure 4: Additional qualitative results on LVU datasets [11]. Five example scenes with their ground truth genre labels as well as our predictions are shown. For example 5, our prediction is different from the label even though looking only at the visual content of this particular scene it makes sense to infer it as a romantic scene. Our hypothesis is that as the genre label of the LVU dataset was acquired from movie-level meta data, sometimes it is not directly applicable to the genre of all of the constituent scenes of a movie.

visual features [9] in Figure 3. We can clearly see that scene-pairs found by our approach are much more thematically meaningful, while the ones found by CLIP focus more on appearance-based similarity and are mostly related to human faces, which are not sufficiently semantically meaningful in terms of scene understanding. This underscores the effectiveness of our approach on downstream tasks related to semantic scene understanding.

2.2. LVU

We present some additional qualitative results on LVU dataset [11]. Specifically, in Figure 4, we show five example scenes with their ground truth genre in LVU as well as our prediction. We can see that our model was able to capture the feature that is useful for correct genre prediction in most

Figure 5: Six examples from the way-of-speaking prediction task in LVU [11]. Results show that when visual information is sufficient to predict way-of-speaking, our method can perform well, and for cases like example 6, it might be beneficial to add audio modality to further improve the accuracy.

cases. For cases like example 5 on the last row, we assume it is because it is sometimes difficult to identify genre from just one scene in the movie, and since the meta information like genre in LVU was retrieved from IMDB entries [11], they cannot always reflect the genre of a specific scene.

In Figure 5, we show six examples from the way-of-speaking prediction task in LVU. We can see that when the visual information is sufficient to make predictions, our model can perform well, but for cases like example 6 on the last row, it can be insufficient to predict just based on visual cues, and this might indicate that for tasks like way-of-speaking prediction, it may be beneficial to include audio modality for better accuracy. This also corresponds to the



Figure 6: Examples of relationship prediction task in LRU [11]. Sometimes the relationship can be ambiguous when there are more than two leading characters in the scene. Also, the uncertainty of some relationships makes prediction even more challenging. For example, it can be difficult to distinguish husband wife and boyfriend girlfriend without semantically understanding of context and plot.

results in Table 2 of the main paper, where the accuracy of way-of-speaking is apparently lower than other tasks. For relationship prediction task in Figure 6, we can see that the model may make ambiguous predictions when there are more than one pair of characters in the scene, and this may indicate that when analyzing relationship in scenes, it might be helpful to focus more on leading characters in that scene for better results.

2.3. MovieNet

We present qualitative results on MovieNet [6] [10] dataset in Figure 7. This corresponds to Table 3 and Table 4 in the main paper and includes examples on place tagging as well as scene boundary detection (SBD) tasks. We show three examples from test set of MovieNet, and in each example, there are two scenes divided by the green dotted line. For each scene, the task is to predict what are the multi-label place tags of the scene, and for the two scenes together, the goal is to predict whether the shot boundaries between each pair of shots are also scene boundaries.

We can see that for SBD, our model can perform well to clearly identify the scene boundaries. For place tagging, it is a much more difficult task involving holistic understanding of the scenes, and although our model outperformed existing state-of-the-art models by a large margin in Table 3 in the main paper, it is still a really challenging and unsolved

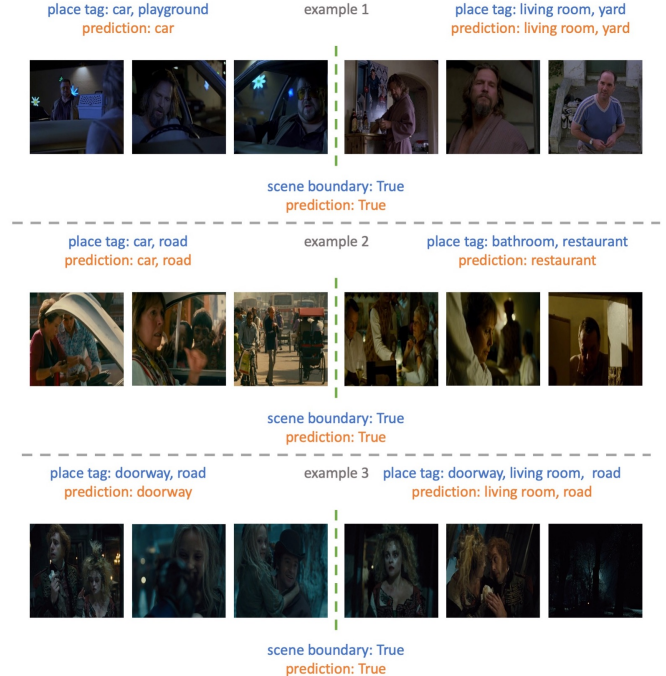


Figure 7: Qualitative results on MovieNet place tagging [6] and scene boundary detection tasks [10]. Although our model outperformed existing state-of-the-art models by a large margin in Table 3 in the main paper, multi-labeled place tagging is still a really challenging problem. Some tags may not be apparent and the intra-category variance is large in this task.

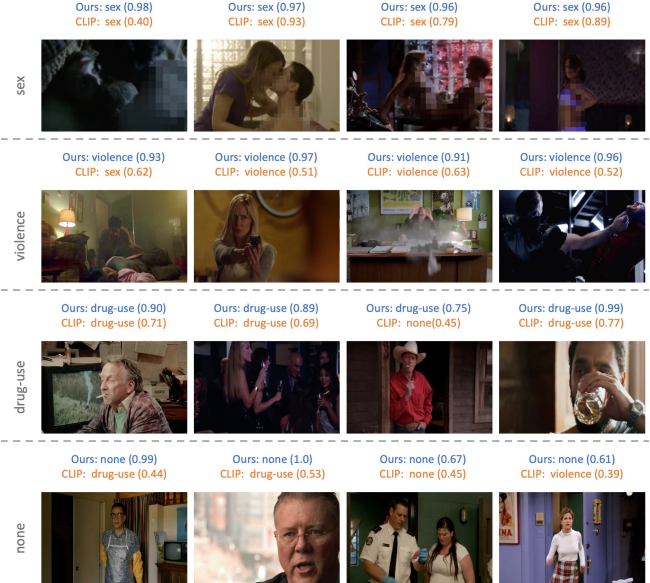


Figure 8: Representative examples in MCD comparing the predictions based on our representation with CLIP visual feature. Sensitive parts of some images are intentionally redacted here.

task. For example, some places are not easy to identify based on a few frames (e.g. playground), and some places can vary a lot in term of appearance but have same place tag (e.g. car). This is also partially caused by the lack of labeled data, where for the 90-category multi-label problem, there are $19.6K$ place tags, with $\sim 11.7K$ for training, leading to ~ 130 labeled training tags per category on average.

2.4. MCD

We present representative examples for each of the 4 classes of our MCD dataset in Figure 8 along with the corresponding detection results (i.e., the class with maximum probability) from both our model and CLIP model. For sex examples, we can see that our model has higher confidence scores compared to CLIP model especially when the images have dark illumination. For violence, the CLIP model sometimes mistakes scenes with two closed persons as sex as shown in the first example. Similarly for drug-use examples, our model classifies them more confidently, and CLIP model misses the small cigarette in the third example and classifies it as none. The none examples show that the CLIP model often mistakes them with other classes, such as violence and drug-use, while our model is able to classify them correctly. This indicates our scene representation performs better than CLIP on age-appropriate activities, demonstrating the effectiveness of our representation in video moderation.

References

- [1] Alexey Dosovitskiy, Lucas Beyer, Alexander Kolesnikov, Dirk Weissenborn, Xiaohua Zhai, Thomas Unterthiner, Mostafa Dehghani, Matthias Minderer, Georg Heigold, Sylvain Gelly, Jakob Uszkoreit, and Neil Houlsby. An image is worth 16x16 words: Transformers for image recognition at scale. *ICLR*, 2021. [2](#)
- [2] Christoph Feichtenhofer. X3d: Expanding architectures for efficient video recognition. In *CVPR*, 2020. [2](#)
- [3] Christoph Feichtenhofer, Haoqi Fan, Jitendra Malik, and Kaiming He. Slowfast networks for video recognition. In *ICCV*, 2019. [2](#)
- [4] Priya Goyal, Piotr Dollár, Ross Girshick, Pieter Noordhuis, Lukasz Wesolowski, Aapo Kyrola, Andrew Tulloch, Yangqing Jia, and Kaiming He. Accurate, large minibatch sgd: Training imagenet in 1 hour. *arXiv:1706.02677*, 2017. [2](#)
- [5] Kaiming He, Haoqi Fan, Yuxin Wu, Saining Xie, and Ross Girshick. Momentum contrast for unsupervised visual representation learning. In *CVPR*, 2020. [2](#)
- [6] Qingqiu Huang, Yu Xiong, Anyi Rao, Jiaze Wang, and Dahua Lin. Movienet: A holistic dataset for movie understanding. In *ECCV*, 2020. [1, 6](#)
- [7] Diederik P Kingma and Jimmy Ba. Adam: A method for stochastic optimization. *arXiv:1412.6980*, 2014. [2](#)
- [8] Adam Paszke, Sam Gross, Francisco Massa, Adam Lerer, James Bradbury, Gregory Chanan, Trevor Killeen, Zeming Lin, Natalia Gimelshein, Luca Antiga, Alban Desmaison, Andreas Kopf, Edward Yang, Zachary DeVito, Martin Raison, Alykhan Tejani, Sasank Chilamkurthy, Benoit Steiner, Lu Fang, Junjie Bai, and Soumith Chintala. Pytorch: An imperative style, high-performance deep learning library. In *NeurIPS*, 2019. [1, 2](#)
- [9] Alec Radford, Jong Wook Kim, Chris Hallacy, Aditya Ramesh, Gabriel Goh, Sandhini Agarwal, Girish Sastry, Amanda Askell, Pamela Mishkin, Jack Clark, et al. Learning transferable visual models from natural language supervision. *arXiv:2103.00020*, 2021. [1, 2, 3, 4, 5](#)
- [10] Anyi Rao, Lining Xu, Yu Xiong, Guodong Xu, Qingqiu Huang, Bolei Zhou, and Dahua Lin. A local-to-global approach to multi-modal movie scene segmentation. In *CVPR*, 2020. [1, 6](#)
- [11] Chao-Yuan Wu and Philipp Krahenbuhl. Towards long-form video understanding. In *CVPR*, 2021. [1, 2, 5, 6](#)